28P

THREE-DIMENSIONAL GUIDANCE EQUATIONS FOR QUASI-OPTIMUM SPACE MANEUVERS

By
Donald J. Jezewski
NASA Manned Spacecraft Center
Houston, Texas, U.S.A.

Presented at the
XVth International Astronautical Congress
Warsaw, Poland
September 7-12, 1964

THREE-DIMENSIONAL GUIDANCE EQUATIONS FOR QUASI-OPTIMUM SPACE MANEUVERS

By Donald J. Jezewski

INTRODUCTION

.29518

An analytical technique has been derived by operating on a set of linearized two-body equations (ref. 1) with the classical calculus of variations to determine a guidance law. A three dimensional case, in which aerodynamic forces are neglected, is treated. The solution differs from that derived in reference 2 in that a continuous constant thrust rather than a constant acceleration is assumed. The equations are first reduced to a flat-body set in two dimensions to determine what approximations may be made and still obtain a valid solution for a class of launch and landing trajectories. By integration, three simultaneous transcendental equations in three unknowns can be derived from this set of equations. The downrange coordinate was assumed to be free at the terminal time. Trajectories resulting from this set are compared with optimum trajectories to determine what errors are present and which terms, deleted by the flat-body approximation, are the principal contributors to the error. Suitable approximate expressions are introduced to the flat-body set of equations to simulate the deleted terms in an attempt to reduce these errors. The equations are again integrated, and the results are compared with the optimum for a number of trajectories. The technique is extended to the three dimensional case, and five independent constants are generated to satisfy the five constraint equations. Guided solutions for launches and landings are illustrated by using the analytic solution as a feedback to the exact integrated mode. Variations in the times of correction are investigated to determine the error incurred as a function of step size.

auth.

The author wishes to acknowledge the assistance of Mr. James Raney and Mr. Ray Roten of the Computation and Analysis Division, NASA Manned Spacecraft Center, who obtained the time-optimum trajectory data for purposes of comparison.

SYMBOLS

A_0	initial thrust acceleration, T/m_0, ft/sec^2
A_z	azimuth angle of velocity, measured positive from north, deg
$a_1, a_2, \ldots, a_n$	coefficients of time series
a_v, a_u, a_w	components of acceleration defined by equations (59), (60), and (61), ft/sec^2
B_0	constant of integration defined by equation (24)
$b_1, b_2, \ldots, b_n$	coefficients of time series
C_0	constant of integration defined by equation (56)
$C_2, C_3, \ldots, C_6$	initial values of Lagrange multipliers, radians/sec
D_0	constant of integration defined by equation (57)
$F_1, F_2, \ldots, F_5$	transcendental functions
g	gravitational acceleration, ft/sec^2
$h_1, h_2, \ldots, h_n$	coefficients of time series
I_{sp}	specific impulse, sec
i	inclination of orbital plane with respect to inertial reference frame, deg
K	constant defined by equations (28) and (29)
k	function defined by equation (26)
L	function defined by equation (58)
M	function defined by equation (25)

m	mass of vehicle, slugs
N	function defined by equation (37)
r	radius to vehicle from center of body, ft
r_0	radius of the reference body, ft
T	thrust, lb
t	time, sec
u,v,w	components of total velocity in x, y, and z directions, respectively, ft/sec
V	total velocity, ft/sec
V_c	characteristic velocity, ft/sec
W	weight of vehicle, lb
X,Y,Z	inertial reference frame, ft
x,y,z	rotating coordinates of vehicle, ft
s	tangent of χ
$\alpha_1,\alpha_2,\alpha_5,\alpha_6$	functions defined by equations (22), (21), (45), and (46), respectively
γ	flight-path angle, deg
ΔV_c	change in characteristic velocity, ft/sec
Δi	change in inclination angle, deg
θ	latitude angle of vehicle, deg
μ	normalized mass ratio, m/m_0
φ	longitude angle of vehicle, deg
χ	thrust pitch angle, measured from local horizontal plane, deg
ψ	thrust yaw angle, measured positive from east, deg

Subscripts:

0,1	initial and final values of state and control variables
A	analytic quantity
I	integrated quantity
n	nth order term of time series

Operators:

$(\dot{})$	time differentation
gd( )	Gudermannian

FORMULATION OF THE PROBLEM

The mathematical model employed in this investigation is a mass particle with three degrees of freedom referred to a set of rotating coordinates in which the y-axis is alined along the local vertical, and the plane formed by the x- and z-axes is the local horizon. The axis system and the associated notation are illustrated in figure 1. This axis system was chosen because it is desired to allow the downrange distance (longitude) at the final time $x_1 = x(t_1)$ to be free or unspecified. In the rotating axis system, the velocity vector is located by the two familiar angles, γ and A_z; and the thrust vector, in a similar sense, is located by the two control angles, χ (pitch angle) and ψ. The angles which locate the position-vector in the inertial reference frame are θ and ϕ.

The equations of motion for this model are

$$\dot{x} = u \tag{1}$$

$$\dot{y} = v \tag{2}$$

$$\dot{z} = w \tag{3}$$

$$\dot{u} = -u(v - w \tan\theta)/r + \frac{A_0}{\mu} \cos\chi \cos\psi \tag{4}$$

$$\dot{v} = (u^2 + w^2)/r - g + \frac{A_0}{\mu} \sin\chi \tag{5}$$

$$\dot{w} = -(vw + u^2 \tan\theta)/r + \frac{A_0}{\mu} \cos\chi \sin\psi \tag{6}$$

where

$$A_0 = T/m_0 \tag{7}$$

$$\mu = 1 + \dot{\mu}t \qquad (0 \le t \le t_1) \tag{8}$$

$$\dot{\mu} = \dot{m}/m_0 \qquad (\dot{m} \le 0) \tag{9}$$

$$g = g_0 \left(r_0/r\right)^2 \tag{10}$$

$$r = \sqrt{X^2 + Y^2 + Z^2} \tag{11}$$

The quantities u, v, and w are the velocity components along the x-, y-, and z-axis, respectively.

The vehicle is assumed to have a constant thrust T and a mass flow rate $\dot{\mu}$ which has been normalized. The initial thrust-to-mass ratio of the vehicle is A_0. The final time t_1 was selected to be minimized since, under the above assumptions, it yields a minimum fuel consumption.

Equations (1) to (11) are, of course, nonlinear, and any attempt to operate on them with the calculus of variations would yield an adjoint set which are also nonlinear.

The problem in the plane is solved first by using the following equations of motion

$$\dot{x} = u \tag{12}$$

$$\dot{y} = v \tag{13}$$

$$\dot{u} = \frac{A_0}{\mu} \cos\chi - uv/r \tag{14}$$

$$\dot{v} = \frac{A_0}{\mu} \sin\chi - g + u^2/r \tag{15}$$

Further, if the radius of the attracting body is allowed to approach infinity, the coupling effects in these equations vanish and the gravitational acceleration approaches the surface value g_0.

The following pitch-angle relationship from reference 2 is obtained when the calculus of variations is applied to this reduced set of equations when the final range is allowed to be free:

$$\tan \chi = \frac{C_4 - C_2 t}{C_3} \tag{16}$$

where the values of C are constants to be determined.

To determine a unique solution, the constants C must be found as functions of the desired boundary conditions. This result is accomplished by integrating the constraint equations between the bounds specified at $t = 0$ and $t = t_1$. The constants C_4/C_3 and C_2/C_3 are obtained by evaluating the pitch-angle relationship at the boundaries and yield

$$\left.\begin{aligned} \frac{C_4}{C_3} &= \tan \chi_0 \\ \frac{C_2}{C_3} &= \frac{\tan \chi_0 - \tan \chi_1}{t_1} \end{aligned}\right\} \tag{17}$$

where $\chi_0 = \chi(0)$ and $\chi_1 = \chi(t_1)$.

Integration of the flat-body equations results in the following three simultaneous transcendental equations in the three unknowns χ_0, χ_1, and t_1.

$$\mu_1 v_1 - \dot{\mu} y_1 - g_0 t_1 \left(1 + \frac{\dot{\mu} t_1}{2}\right) - \frac{\alpha_2}{\dot{\mu}} \left(A_0 \sec \chi_1 - B_0\right) = 0 \tag{18}$$

$$y_1 - \mu_1 y_0 + \frac{g_0 t_1^2}{2\mu_1} - B_0 t_1 - \frac{A_0 \mu_1 K}{\dot{\mu}^2} \left[gd(\chi_1) - gd(\chi_0) + K\alpha_2 N - \frac{K\dot{\mu}\alpha_1}{A_0 \alpha_2} (u_1 - u_0) \right] = 0 \tag{19}$$

$$\frac{Kk^{1/2}\dot{\mu}}{A_0\alpha_2}(u_1 - u_0) - \log_e M = 0 \tag{20}$$

where

$$\alpha_2 = \frac{\dot{\mu}t_1}{\tan \chi_1 - \tan \chi_0} \tag{21}$$

$$\alpha_1 = 1 - \alpha_2 \tan \chi_0 \tag{22}$$

$$gd(\chi) = \log_e(\tan \chi + K \sec \chi) \tag{23}$$

$$B_0 = -\frac{\dot{\mu}}{\alpha_2}(v_0 - \dot{\mu}y_0) + A_0 \sec \chi_0 \tag{24}$$

$$M = \frac{k - \alpha_1\mu_1 - \alpha_2 K\sqrt{k} \sec \chi_1}{k - \alpha_1 - \alpha_2 K\sqrt{k} \sec \chi_0} \tag{25}$$

$$k = \alpha_1^2 + \alpha_2^2 \tag{26}$$

$$N = \sec \chi_0 - \sec \chi_1/\mu_1 \tag{27}$$

$$K = 1 \quad (-\pi/2 \leq \chi \leq \pi/2) \tag{28}$$

$$K = -1 \quad (\pi/2 < \chi < 3\pi/2) \tag{29}$$

Because the control quantities occur implicitly in this set of equations, it is impossible to solve for them directly. Since the equations are transcendental, a first-order perturbation technique (ref. 3) is used to force the solution to converge. This technique, which generates a partial matrix, assumes that a solution exists if the matrix of partials has an inverse.

A solution of this system of equations as compared with that of an optimum integrated round body is indicated in figure 2. The curve shows the variation of characteristic velocity error with initial thrust-to-weight ratio for a launch to lunar orbit.

It should be noted that the error generally decreases with increasing T/W_0. This follows logically since burning time $t_1 \propto (T/W_0)^{-1}$ and as the burning time approaches zero, the surface integrated over approaches a flat body. The solution does not approach zero for increasing values of thrust-to-weight ratio since it is an initial boundary-value solution and not a guided trajectory to the terminal conditions.

The question of what can be done to improve this solution without destroying the analytic properties of the problem is now posed. Certainly, the errors are the result of neglecting the cross-coupling effects and setting g equal to a constant.

Figures 3(a) and 3(b) illustrate time histories of the nonlinear terms

$$a_u = uv/r \tag{30}$$

$$a_v = - g + u^2/r \tag{31}$$

for a minimum-time optimum launch to lunar orbit as compared with those of the flat-body approximations. The displacement between the curves in figures 3(a) and 3(b) represents the horizontal and normal acceleration errors of the flat-body approximation and amounts to a maximum of 5.5 ft/sec^2 for the normal component at the terminal point. The horizontal acceleration term a_u for optimum time descents or ascents from orbit can be considered to have only a second-order effect. For the case illustrated, a launch to lunar orbit, the maximum value of this term amounts to less than 0.2 ft/sec^2. Therefore, the quantity a_v accounts for the largest portion of the observed error.

To offset the errors, functions are defined in the form

$$a_u = \sum_{n=0}^{l} h_{n+1} t^n \tag{32}$$

$$a_v = \sum_{n=0}^{l} a_{n+1} t^n \tag{33}$$

which have the same values as the functions defined in equations (30) and (31) at the two bounds. The introduction of a power series in one of the dependent variables would necessarily complicate (if not completely destroy) the guidance law stated in equation (16). A time series is acceptable because it will not alter the guidance law but will only change the transversality condition of the calculus of variations.

By replacing the nonlinear terms in the two-dimensional model with these time series, the system of equations is integrated by using the control law derived for the flat body. The resulting three simultaneous transcendental equations are solved by the method outlined for the flat-body case. This solution has the added complication of determining the constants of the power series approximation.

The number of coefficients required to simulate sufficiently the nonlinear trajectories is determined by qualitatively examining the time histories of the deleted nonlinear terms. Since an inversion of a matrix of the order of the number of coefficients minus one is involved, it is desirable to retain a minimum number of terms. For the ascent and descent trajectories which were examined, polynomials of the third degree were found to be sufficient. The evaluation of the power-series coefficients was determined by using the information on the present and past history of the state and control variables. Initially, the coefficients are either set equal to zero (other than the first term) or approximated by a backward integration process.

A comparison of this solution with the flat-body approximation and the strict optimum is indicated in figures 3(a) and 3(b). The dashed curve is the power series approximation using a truncated series with four coefficients. The error in the normal acceleration term has been reduced to a negligible amount, and the horizontal term strongly resembles the strict optimum. The time history of the control programs and the terminal values of the state variables for this launch to lunar orbit are presented in figure 4 and table I. In these solutions, the nonlinear equations were integrated at a step interval of 2.5 seconds, and the analytic solution was used as a feedback control. Errors exist in the state variables at the terminal time as a result of the correction interval and the singular nature of the guidance equations as time to go approaches zero. An open-loop system was required for the last portion of the trajectory. A time-history comparison of the state variables of the analytic and optimum integrated solutions would not be of interest since the two sets of curves are nearly coincident.

If the simplifying assumptions of this two-dimensional model are extended to that of the problem originally stated, the equations of motion are reduced to the following form.

$$\dot{x} = u \tag{34}$$

$$\dot{y} = v \tag{35}$$

$$\dot{z} = w \tag{36}$$

$$\dot{u} = \sum_{n=0}^{l} h_{n+1} t^n + \frac{A_0}{\mu} \cos \chi \cos \psi \tag{37}$$

$$\dot{v} = \sum_{n=0}^{l} a_{n+1} t^n + \frac{A_0}{\mu} \sin \chi \tag{38}$$

$$\dot{w} = \sum_{n=0}^{l} b_{n+1} t^n + \frac{A_0}{\mu} \cos \chi \sin \psi \tag{39}$$

The constants a, b, and h are determined by the method previously outlined.

By applying the calculus of variation to this system of equations, minimizing the final time, and once again allowing the final value of x, or the longitude, to be free, the following control-angle relationships result:

$$\tan \chi = \frac{(C_5 - C_2 t)\cos \psi}{C_4} \tag{40}$$

$$\tan \psi = \frac{C_6 - C_3 t}{C_4} \tag{41}$$

The solution is now complete since five independent constants exist to satisfy the five constraint equations. Equation (34) is not integrated since its final value is to be unspecified. The presence of the coupling term $\cos \psi$ in the χ control law increases the difficulty of integrating the linearized equation. Elimination of $\cos \psi$ reduces the interrelationship of the control variables as indicated in the following equations:

If

$$\cos \psi \approx 1, \quad \tan \psi \approx \sin \psi \tag{42}$$

then,

$$\tan \chi = \frac{C_5 - C_2 t}{C_4} = s \tag{43}$$

$$\sin \psi = \alpha_5 + \alpha_6 s \tag{44}$$

where:

$$\alpha_5 = \frac{(C_2 C_6 - C_3 C_5)}{C_2 C_4} \tag{45}$$

$$\alpha_6 = \frac{C_3}{C_2} \tag{46}$$

$$\frac{C_5}{C_4} = \tan \chi_0 \tag{47}$$

$$\frac{C_2}{C_4} = \frac{\tan \chi_0 - \tan \chi_1}{t_1} \tag{48}$$

$$\frac{C_6}{C_4} = \sin \psi_0 \tag{49}$$

$$\frac{C_3}{C_4} = \frac{\sin \psi_0 - \sin \psi_1}{t_1} \tag{50}$$

If ψ is assumed to be small so that $\cos \psi \approx 1$ and $\tan \psi \approx \sin \psi$, it can be observed that although ψ is functionally dependent on χ, the inverse relationship has been eliminated. This can be noted in the term α_6 where C_3/C_2 is the ratio of the control-angle rates. It is shown subsequently how a weaker coupling relationship still exists in the constants of the power series expansion.

The small angle approximation of ψ may at first appear to be an unusually severe restriction until the type of problem to be solved is considered. Lunar landings and launches are to occur at latitudes between $\pm 10^{\circ}$ and azimuth angles of near $\pm 90^{\circ}$. Since large plane changes are not expected, the assumptions and equations stated here are quite valid.

When equations (35) to (39) have been integrated from time $t = 0$ to $t = t_1$, and a considerable amount of manipulation has been performed, the following five transcendental equations in the five unknowns χ_0, χ_1, ψ_0, ψ_1, and t_1 are derived. The method of solution of these equations is as outlined for the two-dimensional flat-body problem.

$$F_1 = \log_e M - \frac{\dot{\mu}\sqrt{kL}}{\alpha_2 A_0} = 0 \tag{51}$$

$$F_2 = \alpha_2(A_0 \sec \chi_1 - C_0) - \dot{\mu}\left\{\mu_1 v_1 - \dot{\mu} y_1 - \sum_{n=0}^{l} \frac{a_{n+1} t_1^{n+1}}{n+1}\left[1 + \frac{\dot{\mu} t_1 (n+1)}{n+2}\right]\right\} = 0 \tag{52}$$

$$F_3 = \dot{\mu}\left\{\dot{\mu}\left[\mu_1 y_0 - y_1 + \sum_{n=0}^{l} \frac{a_{n+1} t_1^{n+2}}{(n+1)(n+2)}\right] - \alpha_2 C_0 t_1\right\} + A_0 \mu_1 \left[gd(\chi_1) - gd(\chi_0) + \alpha_2 N - \frac{\dot{\mu}\alpha_1 L}{A_0 \alpha_2}\right] = 0 \tag{53}$$

$$F_4 = \alpha_2\left\{A_0\left[\alpha_5\, gd(\chi_1) + \alpha_6\, gd(\chi_0)\right] - D_0\right\} + \dot{\mu}\left\{\dot{\mu} z_1 - \mu_1 w_1 + \sum_{n=0}^{l} \frac{b_{n+1} t_1^{n+1}}{n+1}\left[1 + \frac{\dot{\mu} t_1 (n+1)}{n+2}\right]\right\} = 0 \tag{54}$$

$$F_5 = \dot{\mu}\left\{\dot{\mu}\left[\mu_1 z_0 - z_1 + \sum_{n=0}^{l} \frac{b_n t_1^{n+2}}{(n+1)(n+2)}\right] - \alpha_2 D_0 t_1\right\} + A_0\mu_1\left[\alpha_2\alpha_6 N - \left(\frac{\alpha_2\alpha_5}{\mu_1} - \alpha_6\right) gd(\chi_1) + (\alpha_2\alpha_5 - \alpha_6)\, gd(\chi_0) + \frac{\dot{\mu}L}{A_0\alpha_2}(\alpha_2\alpha_5 - \alpha_1\alpha_2)\right] = 0 \tag{55}$$

where

$$C_0 = \frac{\dot{\mu}(\dot{\mu}y_0 - v_0)}{\alpha_2} + A_0 \sec \chi_0 \tag{56}$$

$$D_0 = \frac{\dot{\mu}(\dot{\mu}z_0 - w_0)}{\alpha_2} + A_0\left[\alpha_5\, gd(\chi_0) + \alpha_6 \sec \chi_0\right] \tag{57}$$

$$L = u_1 - u_0 - \sum_{n=0}^{l} \frac{h_{n+1} t_1^{n+1}}{n+1} \tag{58}$$

As was previously mentioned, if a small angle approximation is made on ψ, the equations of motion appear to be uncoupled at least in one direction. However, for guided trajectories, a weaker coupling relationship exists in the constants of the power-series expansions:

$$a_u = -u(v - w\tan\theta)/r = \sum_{n=0}^{l} h_{n+1} t^n \tag{59}$$

$$a_v = -g + (u^2 + w^2)/r = \sum_{n=0}^{l} a_{n+1} t^n \tag{60}$$

$$a_w = -(vw + u^2\tan\theta)/r = \sum_{n=0}^{l} b_{n+1} t^n \tag{61}$$

Each time the trajectory is corrected, the power-series constants are corrected on the basis of the present and past state as indicated in equations (59), (60), and (61). The accelerations in the x and y directions are not independent of the acceleration in the z direction but are coupled through the constants a_n and h_n of the power series.

RESULTS

The degree of success achieved by using equations (51) to (58) to simulate the strict optimum can be best shown, under the assumption of no boundary-value errors, by performance data in terms of characteristic velocity. This quantity, for a constant mass-flow rate, is a measure of the amount of fuel consumed. For the two-dimensional case already considered, the launch to lunar orbit, the performance loss is approximately 2 ft/sec with respect to the strict optimum. With this small performance loss, it can be assumed that the state and control variables closely resemble those of the integrated solution. The control angle χ had the most noticeable deviation; the maximum variation was at the initial time and amounted to 1°. Throughout the trajectory, abnormal control angular rates were not encountered; and as time to go approached zero, they were avoided by using an open-loop system.

The trajectories presented in this paper are compared on the basis of performance in terms of characteristic velocity. The strict optimum and analytic control angles are also compared. A table of errors is given for each solution in which the terminal miss errors are indicated as functions of the correction intervals.

Figure 5 is a time-history comparison of the control angles χ and ψ for a descent from a circular lunar orbit with longitude free to a flare maneuver at an altitude of 5,000 feet. The solid curves represent the strict optimum, obtained through integration, and the dashed curves are the analytic approximations. The tendency of the control angle χ to be linearized versions of the optimum is a characteristic of the solution for launches to and from lunar orbits. The agreement in the yaw angle ψ is also very good until the strict optimum has a rapid change in slope at which time the analytic solution only hints at following. The small angle approximation made on ψ in the analysis is verified in this figure. A plane change of 2.8017° was required to satisfy the terminal state vector. Table II lists the state variable errors and performance loss at the terminal time, as compared with the strict optimum for the correction intervals of 2.5, 5.0, and 10.0 seconds. A correction interval is given as the time between corrections of the constants C defined in the analysis. A performance loss of less than 1 ft/sec was obtained for the boundary

conditions listed for the 2.5-second correction interval. This trajectory had an initial thrust-to-weight ratio of 0.4172 and a specific impulse of 314 seconds. The initial and final conditions on the state variables are also listed in the table. The solutions agree very well with the optimum with the largest errors occurring in velocity and azimuth. The apparent large error in γ at the terminal time is the result of a rapid change in this quantity in the last few seconds of the trajectory. Although they are not presented in this paper, results for a flare maneuver in two dimensions with $\gamma_1 = -11°$ compared very well with only a 0.05° error for a correction interval of 10 seconds. Velocity and azimuth angles have apparent minimum errors at the 5-second correction interval whereas the errors in the remaining variables decrease with the decreasing interval.

Figure 6 is the time-history comparison of the control angles χ and ψ for an ascent from the lunar surface to the pericynthion of an orbit which has an eccentricity of 0.0429. The longitude is once again held free. The agreement in pitch angle χ is exceptionally good with the maximum deviation being approximately $\frac{1°}{2}$. This good agreement would be expected a priori since, as mentioned previously in the analysis, a high thrust-to-weight ratio indicates that there is a short burning time and that the surface integrated over approaches a flat body. Under these conditions, the control law derived for the analytic solution more nearly approximates the true optimum. The yaw angle solutions at first appear to be complete opposites until consideration is made of the performed trajectory maneuver. Yaw angle is measured in the same sense as azimuth, and for a launch in which the flight path angle approaches 90°, the azimuth angle is nearly undefined. Therefore, the yaw control angle is poorly defined initially. In order to meet the terminal boundary conditions, the yaw angle of the analytic solution must decrease since initially it had a greater positive value than the strict optimum.

Table III lists the state variable errors and performance loss at the terminal time for the correction intervals of 2.5, 5.0, and 10.0 seconds. The initial and final values of the state variables are also listed in the table. The initial thrust-to-weight ratio was 1.0115, and the specific impulse was 310 seconds. A plane change of 1.3262° was required to meet the terminal conditions. Contrary to the descent trajectory, velocity and azimuth have maximum errors at the 5-second correction interval rather than minimums. The errors in the remaining variables decrease with a decreasing correction interval.

Table IV lists the error data for an optimum insertion into a circular earth orbit. A small plane change of 1.367° was required to satisfy the terminal state vector. An initial thrust-to-weight ratio

of 0.86 and a specific impulse of 426 seconds were used. The initial and final conditions on the state variables are also listed in the table. A performance loss of 239 ft/sec, or 1.28 percent with respect to the strict optimum, was obtained for a correction interval of 2.5 seconds. The errors can be seen to be quite small for a trajectory of this type. They follow the same trend as those for the lunar descent maneuver with velocity having an apparent minimum at a correction interval of 5.0 seconds and the errors in the remaining variable decreasing with a decreasing interval.

CONCLUDING REMARKS

Quasi-optimum guidance equations in three dimensions for which constant thrust was used have been analytically derived by the calculus of variations. The basis of the analysis is the analytical solution to the flat-body problem which is extended to simulate a round body by the addition of power series in time. Numerical solutions to the resulting transcendental equations have been generated by using an iterative convergence technique.

Guided trajectories were examined for a landing on and launch from the lunar surface and for an insertion into earth orbit. The resulting curves for the control angles agree closely with the true optimum and produce solutions which are more linear than the exact curves. Terminal state errors and performance data are presented for the correction intervals of 2.5, 5.0, and 10.0 seconds. The errors in the state variables generally decrease with a decreasing correction interval. For the lunar trajectories, the azimuth angle was difficult to control and had terminal errors of approximately 1 percent; whereas, for the earth-orbital insertion trajectory, the azimuth angle error was two magnitudes smaller.

REFERENCES

1. Jezewski, D. J.: Guidance Equations for Quasi-Optimum Space Maneuvers. NASA TN D-2361, 1964.

2. Lawden, Derek F.: Interplanetary Rocket Trajectories. Volume I of Advances in Space Sciences, ch. I, Frederick I. Ordway, III, ed., Academic Press (New York and London), 1959, p. 8.

3. Margenau, Murphy: The Mathematics of Physics and Chemistry. Ch. XIII, 2nd ed. D. Van Norstrand Co., Inc. (Princeton, N.J.), 1959, p. 493.

TABLE I.- COMPARISON OF TERMINAL CONDITIONS FOR AN OPTIMUM LAUNCH TO LUNAR ORBIT

$\left[T/W_0 = 0.6;\ I_{sp} = 315 \text{ sec};\ y_0 = 1{,}000 \text{ ft};\ V_0 = 100 \text{ ft/sec};\ \gamma_0 = 90^\circ\right]$

	Optimum, integrated	Analytic, guided
V_c, ft/sec	5,772.5	5,774.6
y_1, ft	49,957.9	49,957.4
V_1, ft/sec	5,606.7	5,606.7
γ_1, deg	0.00084	0.00341
φ_1, deg	5.6730	5.6805

TABLE II.- TERMINAL STATE ERRORS FOR GUIDED DESCENT FROM LUNAR ORBIT TO FLARE AT ALTITUDE OF 5,000 FEET – LONGITUDE FREE

Initial conditions		Final conditions	
T/W_0	0.4172		
I_{sp}, sec	314		
V_0, ft/sec	5,685	V_1, ft/sec	100
y_0, ft	50,000	y_1, ft	4,998.4
γ_0, deg	0.0	γ_1, deg	-0.00177
θ_0, deg	-1.532	θ_1, deg	-0.35157
A_{z0}, deg	-83.38	A_{z1}, deg	-87.0
φ_0, deg	-17.93	φ_1, deg	-28.039
Δi, deg	2.8017		

Error	Correction interval, sec		
	2.5	5.0	10.0
V_c, ft/sec	0.93	2.93	5.47
V, ft/sec	1.990	0.949	1.928
y, ft	0.27	0.87	4.83
γ, deg	0.0055	0.2126	1.2326
θ, deg	0.0022	0.0022	0.0022
A_z, deg	0.8809	0.3462	0.9121
φ, deg	0.0157	0.0170	0.0197

TABLE III.- TERMINAL STATE ERRORS FOR GUIDED ASCENT TO LUNAR ORBIT – LONGITUDE FREE

Initial conditions		Final conditions	
T/W_0	1.0115		
I_{sp}, sec	310		
V_0, ft/sec	100	V_1, ft/sec	5,600
y_0, ft	0.0	y_1, ft	50,000
γ_0, deg	85	γ_1, deg	0.0
θ_0, deg	0.9	θ_1, deg	1.4
A_{z0}, deg	80	A_{z1}, deg	81.5
φ_0, deg	-28	φ_1, deg	-24.668
Δi, deg	1.3262		

Error	Correction interval, sec		
	2.5	5.0	10.0
V_c, ft/sec	1.64	3.54	11.56
V, ft/sec	3.63	31.07	7.004
y, ft	0.55	8.47	105.37
γ, deg	0.0009	0.0506	0.0999
θ, deg	0.0006	0.0003	-0.0011
A_z, deg	-0.1013	0.4499	0.0937
φ, deg	0.0003	0.0004	0.0066

TABLE IV.- TERMINAL STATE ERRORS FOR GUIDED INSERTION INTO CIRCULAR EARTH ORBIT – LONGITUDE FREE

Initial conditions		Final conditions	
T/W_0	0.86207		
I_{sp}, sec	426		
V_0, ft/sec	8,100	V_1, ft/sec	25,567
y_0, ft	445,000	y_1, ft	635,000
γ_0, deg	14.3	γ_1, deg	-0.0018
θ_0, deg	15	θ_1, deg	16.502
A_{z0}, deg	80	A_{z1}, deg	88.1932
φ_0, deg	-70	φ_1, deg	-55.328
Δi, deg	1.367		

Error	Correction interval, sec		
	2.5	5.0	10.0
V_c, ft/sec	239.17	249.58	269.63
V, ft/sec	1.89	0.98	3.20
y, ft	0.80	9.00	70.90
γ, deg	0.0052	0.0161	0.0534
θ, deg	0.0047	0.0046	0.0045
A_z, deg	0.0252	0.0262	0.0280
φ, deg	0.0010	0.0050	0.0126

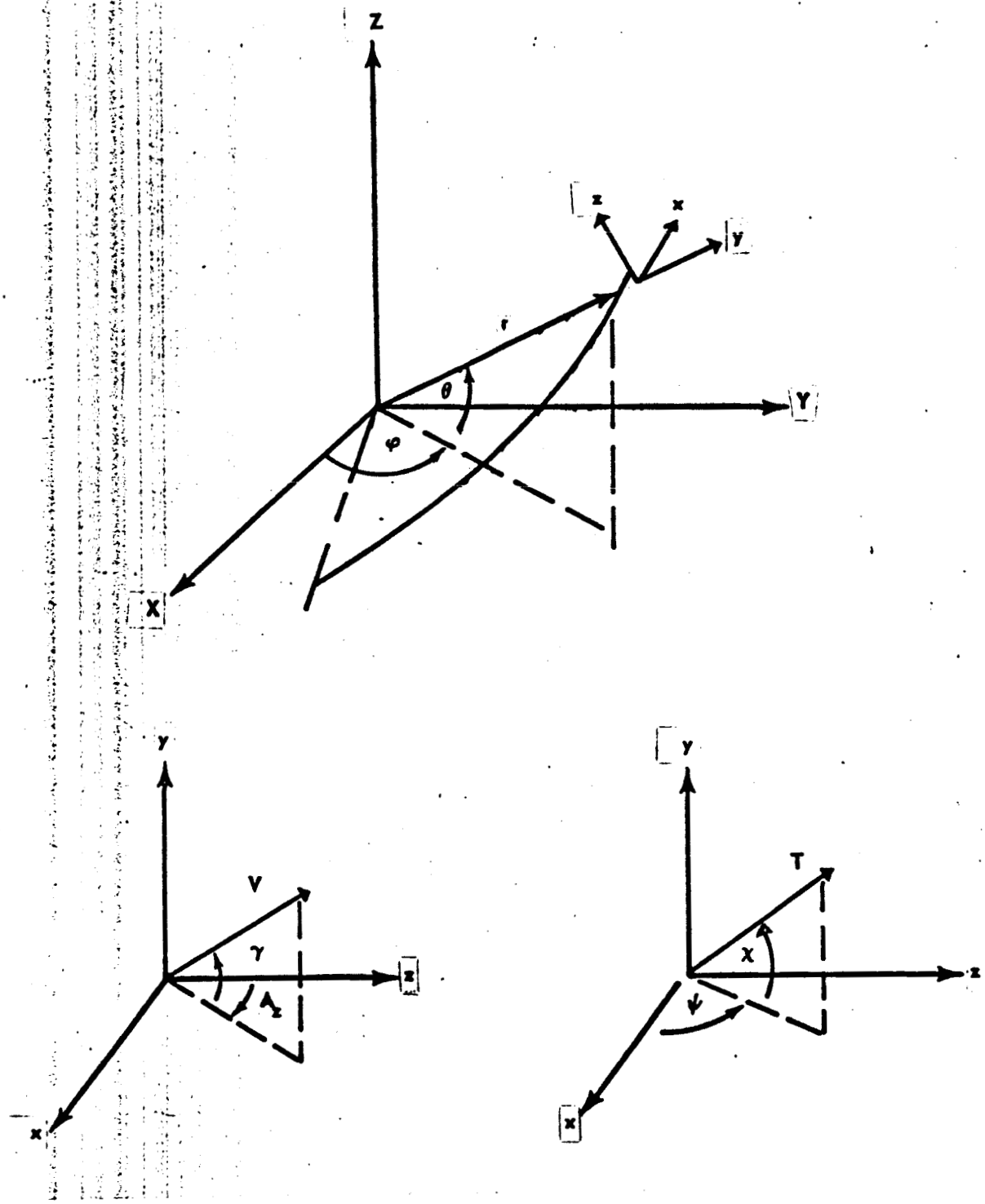

Figure 1.- Coordinate system and angle definition.

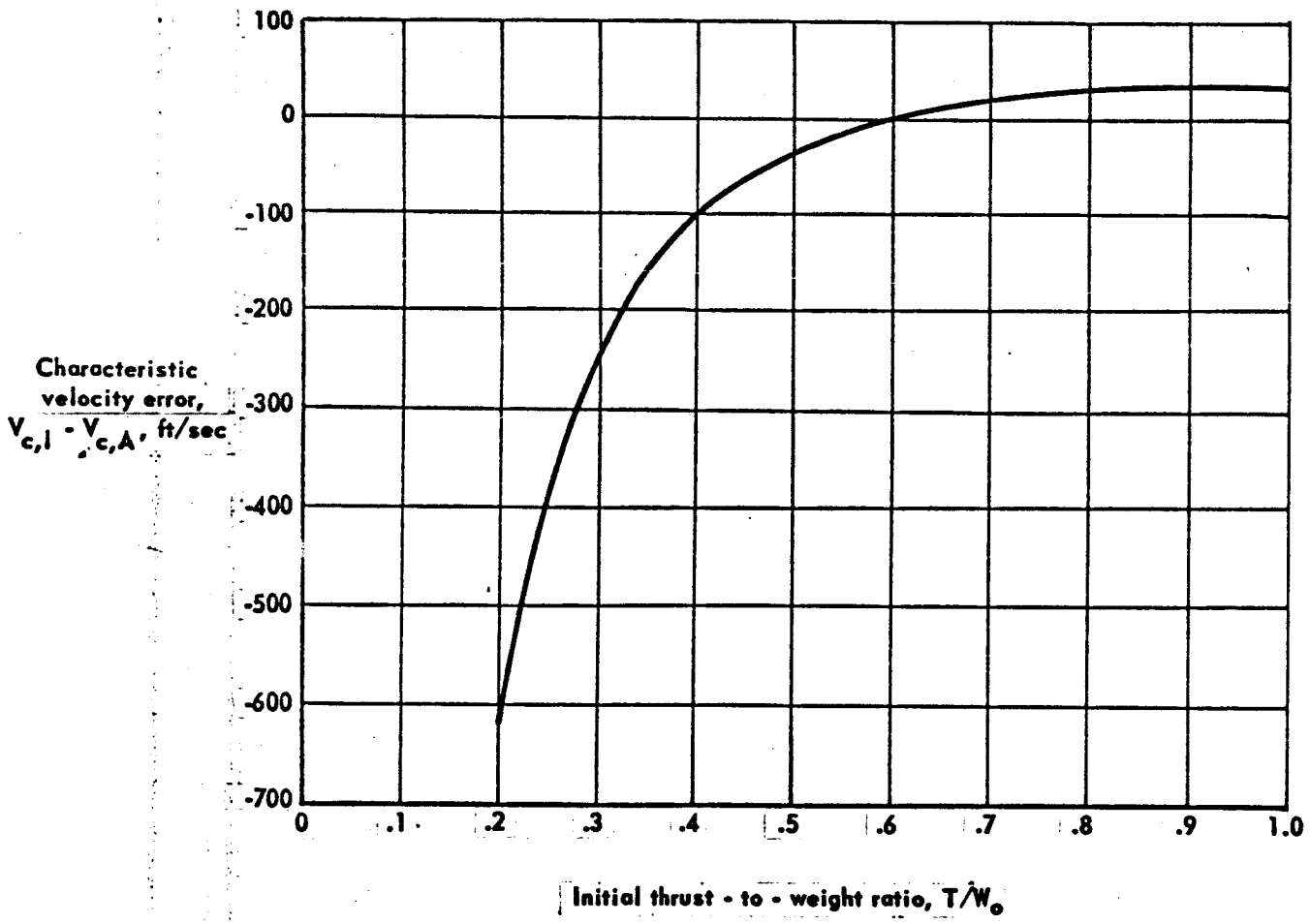

Figure 2.- Flat body characteristic velocity error for a launch to lunar orbit. I_{sp} = 420 sec; g_0 = 5.32 ft/sec^2.

NASA-S-64-283

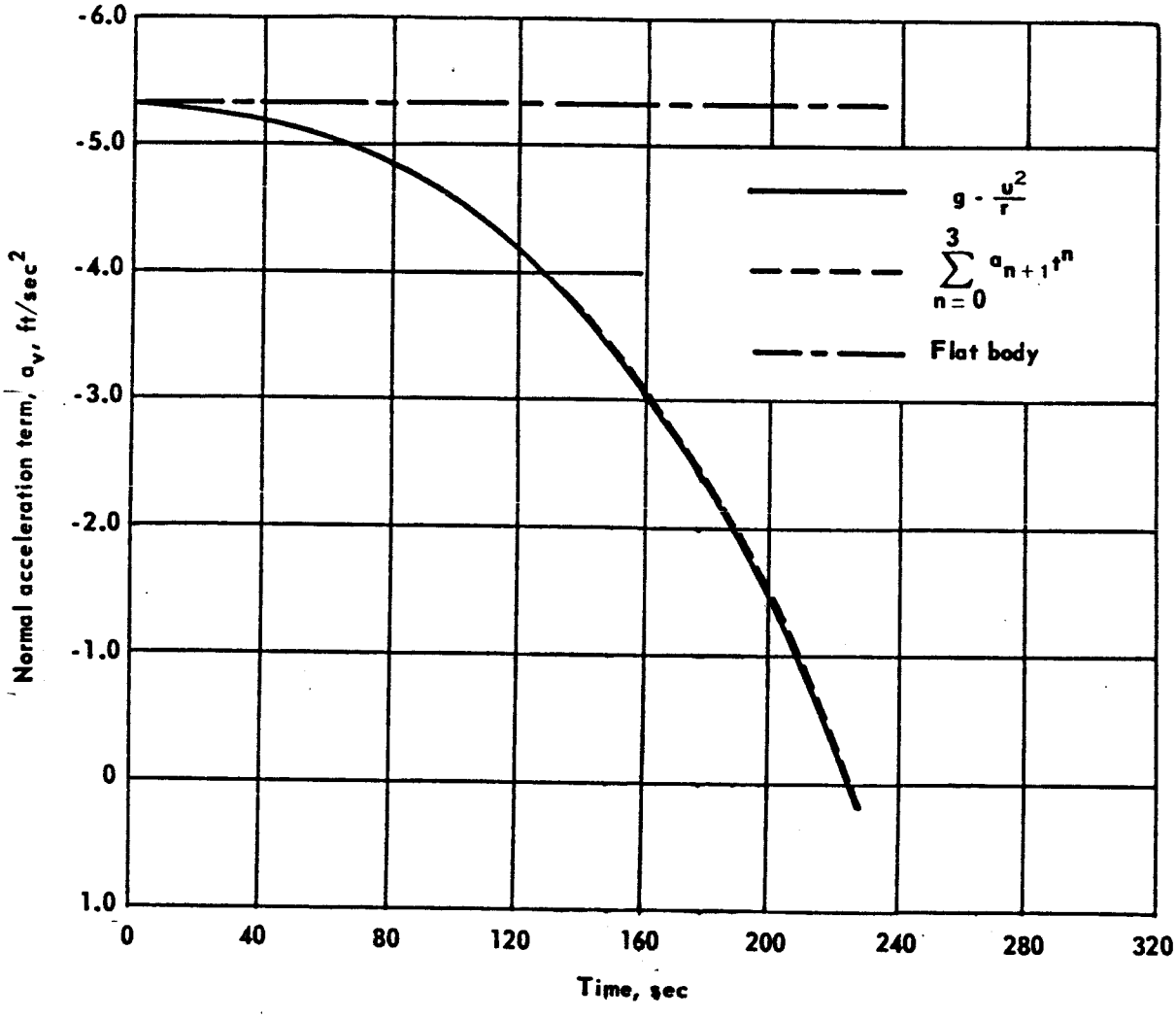

(a) Normal acceleration term.

Figure 3.- Comparison of solution obtained by using analytic and exact solutions for launch to lunar orbit. $T/W_0 = 0.6$; $I_{sp} = 315.0$ sec.

NASA-S-64-282

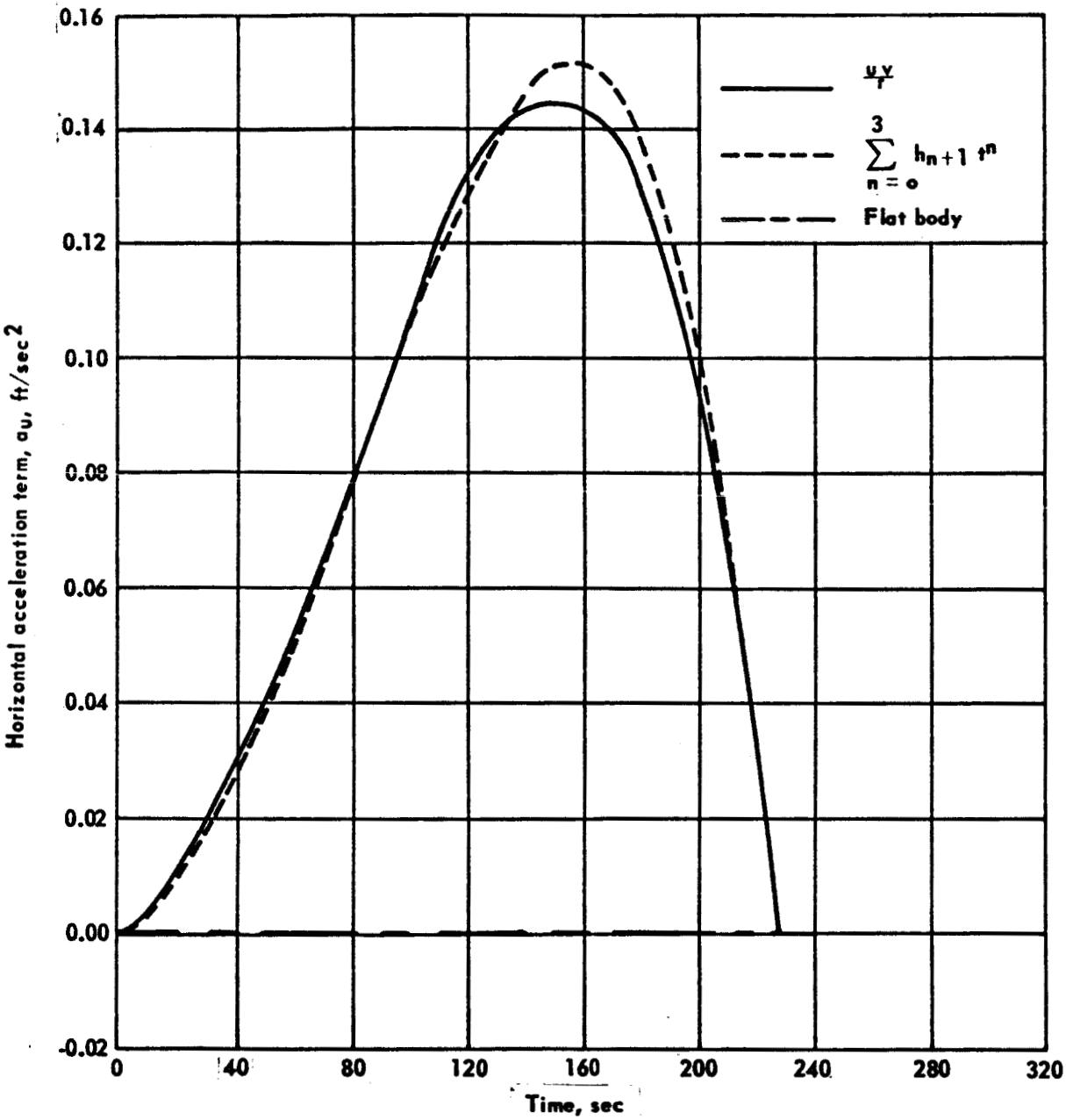

(b) Horizontal acceleration term.

Figure 3.- Concluded.

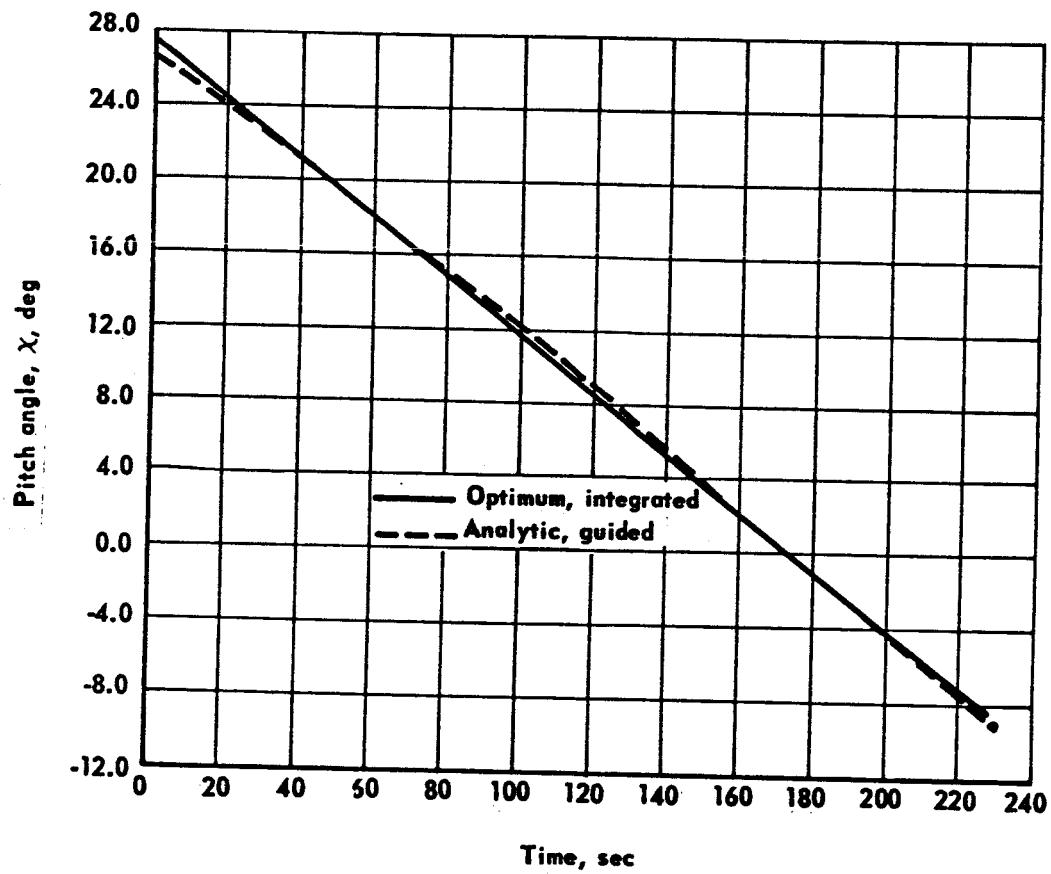

Figure 4.- Optimum launch to lunar orbit.
$T/W_0 = 0.6$; $I_{sp} = 315$ sec.

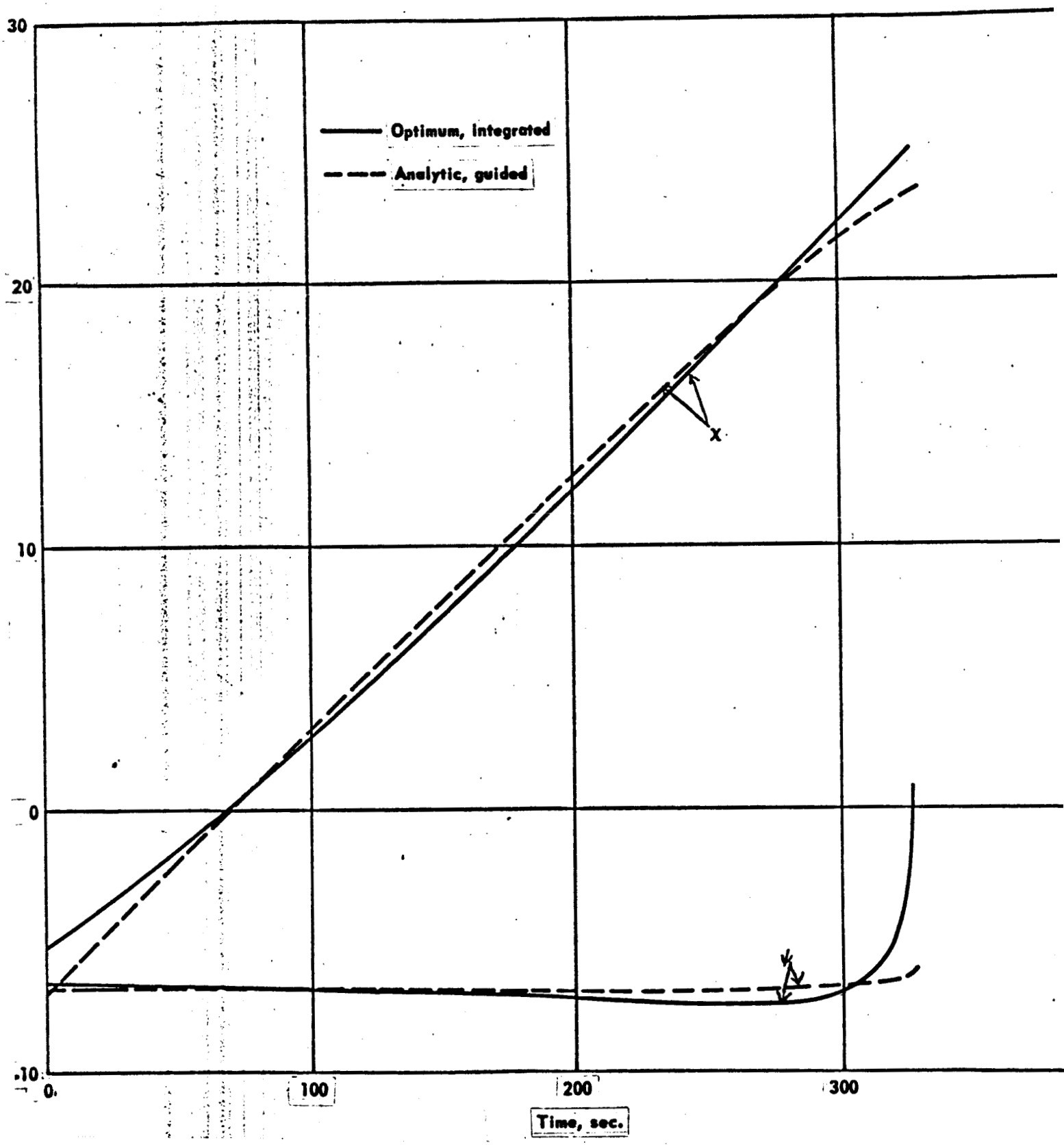

Figure 5.- Optimum descent from lunar orbit with longitude free.

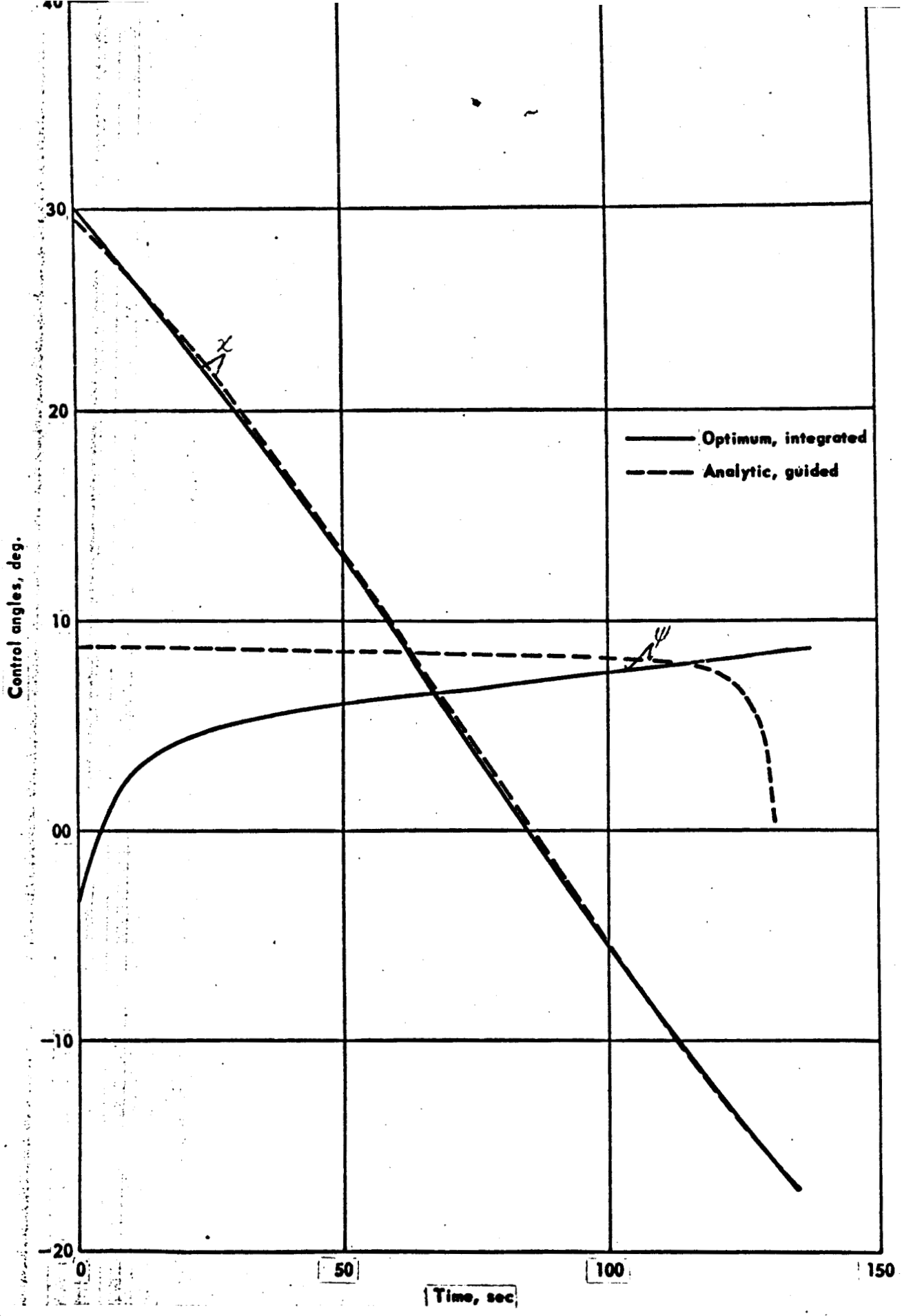

Figure 6.- Optimum ascent to lunar orbit with longitude free.